Method for measuring unstable dimension variability from time series

N. J. McCullen* and P. Moresco†
School of Physics and Astronomy, The University of Manchester, Manchester M13 9PL, United Kingdom
(Received 22 July 2005; revised manuscript received 21 December 2005; published 11 April 2006)

Many of the results in the theory of dynamical systems rely on the assumption of hyperbolicity. One of the possible violations of this condition is the presence of unstable dimension variability (UDV), i.e., the existence in a chaotic attractor of sets of unstable periodic orbits, each with a different number of expanding directions. It has been shown that the presence of UDV poses severe limitations to the length of time for which a numerically generated orbit can be assumed to lie close to a true trajectory of such systems (the shadowing time). In this work we propose a method to detect the presence of UDV in real systems from time series measurements. Variations in the number of expanding directions are detected by determining the local topological dimension of the unstable space for points along a trajectory on the attractor. We show for a physical system of coupled electronic oscillators that with this method it is possible to decompose attractors into subsets with different unstable dimension and from this gain insight into the times a typical trajectory spends in each region.

DOI: 10.1103/PhysRevE.73.046203 PACS number(s): 05.45.Tp, 05.45.−a, 05.45.Gg

I. INTRODUCTION

Dynamical systems theory has proven an invaluable tool for the understanding of systems presenting nonlinear phenomena. It is well known that the solutions of nonlinear ordinary differential equations can exhibit sensitive dependence on initial conditions, or chaos, where two trajectories with close initial conditions diverge exponentially in time from one another. This arises because an attractor of the system contains a dense set of unstable periodic orbits and, on average, the tangent spaces along points of a typical trajectory possess an expanding direction. In dissipative systems with more than three degrees of freedom there can be more than one locally expanding direction, a phenomenon known as *hyperchaos*.

Sensitivity to initial conditions naturally leads to the question of whether the *pseudotrajectories* computed from models of physical systems, which suffer from round-off errors and inaccuracies in the model, actually correspond to some true solution of the system. Research in recent years has yielded sufficient conditions under which true trajectories exist that stay close to, or *shadow*, pseudotrajectories for long times; thus giving validity to statistical values obtained from computed trajectories. The length of time for which these conditions are valid, known as the *shadowing time*, has been shown to be strongly related to the concept of hyperbolicity. The dynamics on the attractor is said to be hyperbolic if the following three conditions are satisfied [[1], p. 238]:

(1) at each point in the set the tangent space can be split into expanding and contracting subspaces, along which the distances between two nearby trajectories will, respectively, grow or shrink exponentially in time;

(2) the angle between the stable and unstable subspaces is bounded away from zero; and

(3) along a typical trajectory the expanding subspaces evolve continuously into expanding subspaces only, and contracting subspaces into contracting ones.

The attractors of only a few dynamical systems can be proved to be hyperbolic for certain parameter values and it is believed that attractors in physically relevant systems usually lose hyperbolicity due to the existence of points violating conditions 2 or 3 [2]. The second condition is violated if a tangency exists between the stable and unstable manifolds at some point on the attractor, where an expanding and contracting direction coincide. The third condition cannot be satisfied if there are variations in the dimension of the expanding and contracting subspaces in different parts of the set. This form of nonhyperbolicity is called unstable dimension variability (UDV).

It is believed that the presence of tangencies is a common feature in low-dimensional systems but in systems with more than three degrees of freedom, where attractors can be hyperchaotic and contain periodic orbits with more than one expanding direction, UDV is believed to be commonplace [3]. It has been shown that for hyperbolic systems the shadowing time is infinite [4], while for systems with tangencies the shadowing time will in general be finite and dependent on the error in each step of the computation of the trajectory [5]. Nevertheless, in many cases, using high accuracy calculations allows for the computation of trajectories long enough to estimate reliable statistical averages. On the other hand, the obstruction to shadowing due to UDV has been found to be especially severe, leading not only to very short shadowing times, but also to a significant amplification of computational errors, suggesting that the modeling and computed averages are highly unreliable in such cases [6–8].

The existence of expanding and contracting directions in phase space is related to positive and negative Lyapunov exponents, respectively. Lyapunov exponents quantify the rate of exponential expansion or contraction of volumes over the whole of a given attractor, and can be calculated by averaging over an infinite trajectory the local expansion and contraction of segments linking nearby points. They can also

*Electronic address: mccullen@reynolds.ph.man.ac.uk
†Electronic address: moresco@manchester.ac.uk

be defined for finite times, giving information on the local rather than global expansion and contraction rates. If a trajectory visits regions of the attractor with a different number of expanding directions, the number of positive short-time Lyapunov exponents (STLEs) will also vary. The change in sign of one or more of the STLEs is usually used in numerical experiments to detect the presence of UDV and the associated obstruction to shadowing [6].

When faced with a real physical system, information on the presence of UDV will be useful in determining the parameter ranges in which we can expect models and numerical simulations to give results that correspond to real states of the system. One approach would be to use the information provided by STLEs to determine the presence of UDV from the measurements, but the calculation of Lyapunov exponents from experimental data is far more difficult than in the numerical case. The presence of noise and constraints in the amount of data available impose serious limitations on techniques available for this purpose [9]. These difficulties become more acute if we try to obtain STLEs, as the amount of available data is further reduced.

In this work we discuss a method for detecting UDV in experimental data that does not require the calculation of STLEs. The method instead determines the topological dimension of the unstable space for points along a trajectory on the attractor and, hence, it is able to detect variations in the number of expanding directions. Although it also suffers from the presence of noise and a limited amount of data, the fact that we are trying to estimate an integer value rather than to determine the sign of a quantity that can be close to zero makes the method more robust.

The following sections detail our method and some of its applications. In Sec. II we discuss the effect of UDV on the features of an attractor and describe our proposed method for its detection. In Sec. III A we present a physical system of two coupled electronic oscillators, used as a test for our method. The presence of UDV in a model of the system is shown numerically in Sec. III B. In Sec. III C we apply our method to a time series from the experimental system and show the presence of UDV for certain parameter values. We also compare the robustness of our method to that of other approaches.

II. METHOD FOR DETECTING UDV FROM TIME SERIES

It is usually not possible to measure experimentally all the degrees of freedom in a given system simultaneously and techniques have been developed to extract as much dynamical information as possible from available data. One of the principal advances in the field of nonlinear time series analysis has been the realization that information on attractors in the system can be obtained from time series measurements via embedding techniques. The delay-embedding technique of Takens [10] and derived methods [11] provide a reconstruction of the attractor which preserves dynamical properties of the real system such as its fractal dimension and Lyapunov exponents. If $\{w_1, w_2, \ldots, w_N\}$ is a time series of measurements of some smooth function of the state of the system taken at a constant sampling rate, then points x_i in the reconstructed attractor are defined as

$$x_i = (w_i, w_{i+1}, w_{i+2}, \ldots, w_{i+\nu-1}), \tag{1}$$

where ν, the embedding dimension of the attractor, is taken as the lowest dimension in which trajectories do not cross in phase space, as required for any deterministic system. The method described here works on attractors reconstructed from time series data using time-delay embedding.

We will assume that we are dealing with an ergodic attractor $\mathcal{A}$ with an invariant measure σ and contained in a smooth manifold $\mathcal{M}$. For almost every point x in $\mathcal{A}$, the region of $\mathcal{M}$ around x, $\mathcal{M}_x$, can then be described by means of local stable and unstable manifolds and the corresponding linear tangent spaces [12]. This will result in trajectories passing through $\mathcal{M}_x$ being displaced apart along the unstable directions and driven together along the stable directions. Thus the trajectories inside $\mathcal{M}_x$ will be organized in a way that is related to the local structure of the stable and unstable manifolds. Our aim is to determine the dimension of the linear subspace associated to the expanding directions from the distribution of points belonging to these trajectories.

For a large class of systems including axiom *A* attractors the conditional measure induced by σ is smooth on unstable manifolds [13]. On the other hand, due to the complicated folding of the chaotic attractor the measure is fractal along the stable directions. In experimental systems, the finite amount of data and the presence of noise limit the observability of this fractal structure, and locally the distribution of experimental data approximates the subspace spanned by the unstable and neutral (in the direction of the flow) directions, with a certain "thickness" in the stable directions (Fig. 1). So, for example, in the case where there is locally one expanding direction, the set of points will approximate a two-dimensional surface, while for two expanding directions the set of points will be distributed in an approximately three-dimensional volume.

Our aim is to determine from these sets of points the dimension of the local expanding set. The method looks at the local distribution in phase space of points belonging to numerous trajectories and calculates the local topological dimension on which those points sit and from this the number of locally expanding directions.

Several methods have been proposed to determine the local topological dimension of the manifold containing the attractor [14–16]. Although these techniques have a sound theoretical basis, we found certain practical restrictions in their application to our test system. The method of Froehling *et al.* [14] attempts to fit the data to the local tangent space by means of linear regression. This is repeated for increasing dimension of fit, until the correct dimension is determined from the χ^2 values obtained. Thus the method relies upon the linear approximation being valid in the region from which the data are taken, that is, the radius of the local region containing the points must be small enough to ensure minimal curvature. This is in competition with the need for the level of noise in the contracting directions to be small compared to the radius of the set of points under investigation, and with having a region big enough that it contains suffi-

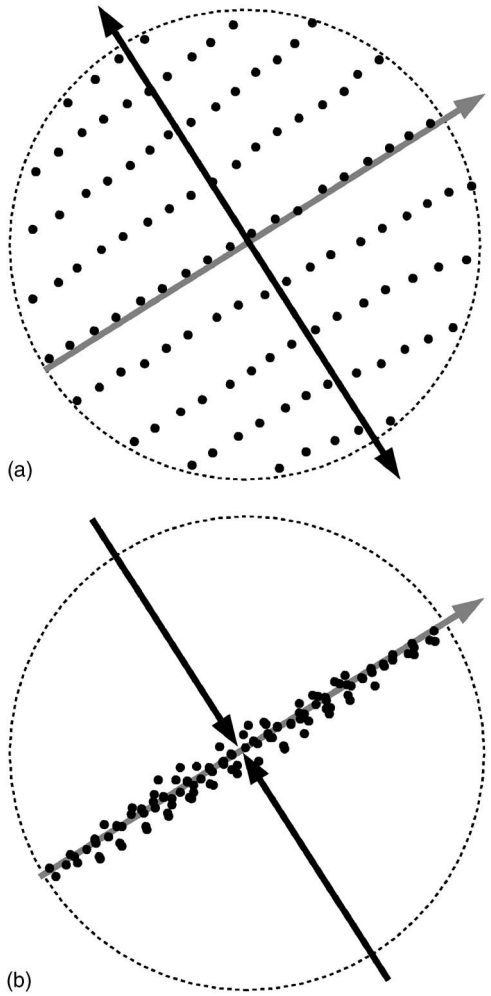

FIG. 1. The distribution of points around a chosen trajectory point. Expanding directions, ←→, and the neutral direction of flow (shaded arrow) show a spread of points, whereas contracting directions, →←, appear almost flat. Thus the dimension of the containing region is strongly related to the number of unstable dimensions.

cient points for the analysis to be reliable. Similar difficulties arise in the technique developed by Broomhead *et al.* [15] and also that of Hediger [16], which make use of singular value decomposition (SVD) to obtain the number of linearly independent vectors locally spanning the tangent space to the manifold containing the attractor. These have proved to be valuable techniques for data analysis, especially determining the dimension of low-dimensional attractors, but in hyperchaotic regimes, such as those found in the system described in Sec. III, we found difficulties in obtaining values which we could interpret easily. We believe this is mainly due to the presence of noise and curvature, as well as a limited amount of data, all of which adversely affect the values obtained.

Instead of the above methods, we decided to use a result by Hammersley [17] on the distribution of distances between points uniformly distributed in a hypersphere. It was shown there that when the number of points is infinite, the mean distance between them converges to a definite value that depends on the dimension, ν, of the hypersphere. We found this result to be useful for determining the dimension of the space containing a given set of points, even if their number is finite and their distribution nonuniform. Although the presence of curvature and noise has a detrimental effect on the values obtained, this way of determining the local dimension of the set appears to be more robust than the other techniques mentioned earlier.

TABLE I. The mean distance between points uniformly distributed in unit diameter hyperspheres of various dimension. Values obtained by Bennet (see Ref. [18]) from a result by Hammersley (see Ref. [17]).

Dimension, ν	Mean, $\mu_\nu(d)$	Variance, $\mathrm{var}_\nu(d)$
1	0.3333	0.05555
2	0.4531	0.04469
3	0.5143	0.03551
4	0.5521	0.02857
⋮	⋮	⋮
∞	0.7071	0.00000

For points uniformly distributed in a hypersphere of dimension ν, the values of the mean interpoint distances $\mu_\nu(d)$ (normalized by the diameter of the hypersphere) and the corresponding variances $\mathrm{var}_\nu(d)$ for several values of ν, were calculated by Bennet [18] and are included in Table I. To evaluate the robustness of the method, we calculated mean distances for numerically generated sets of points, randomly distributed and contained in spaces of a different dimension. The results were so close to the tabulated values as to leave no doubt about the dimension of the space involved. This was also the case when the points contained components in higher dimensions, but whose magnitude was small compared to the other directions. As an example of the robustness of the method, for a two-dimensional unit diameter disk of 800 randomly distributed points, with a thickness in the third direction of 10% of the diameter of the disk, the value of $\mu_\nu(d)$ obtained was 0.4535, which is very close to the value 0.4531 that corresponds to a two-dimensional set. Thus we expect this approach to be successful in cases where data sets are large enough that at each point of the embedded attractor it is possible to define a local region of phase space containing a few hundred points.

Our method for the detection of UDV works by first defining a small hyperspherical region around each point in a long trajectory on the embedded attractor. The distances between all the pairs of points in this neighborhood are measured and their average $[\mu(d)]$ calculated and normalized by the largest recorded distance. This is then repeated for a few successive points along the same trajectory and an average $(\bar{\mu})$ is obtained to smooth out local statistical variations. Once the procedure has been carried out for a long trajectory, visiting most parts of the attractor, a histogram is produced to show the statistics of $\bar{\mu}$ for the whole attracting region. Unstable dimension variability then shows up as multiple peaks in the histogram, each denoting a region with a given number of expanding directions.

In order to test our method, we applied it to numerically generated time series data from the kicked double-rotor sys-

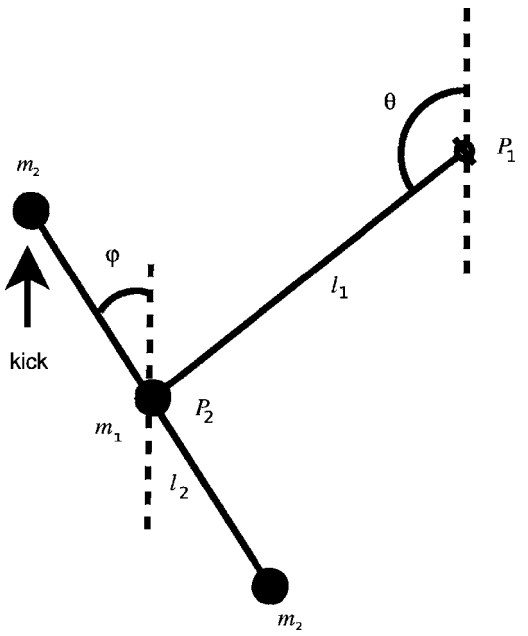

FIG. 2. The kicked double rotor.

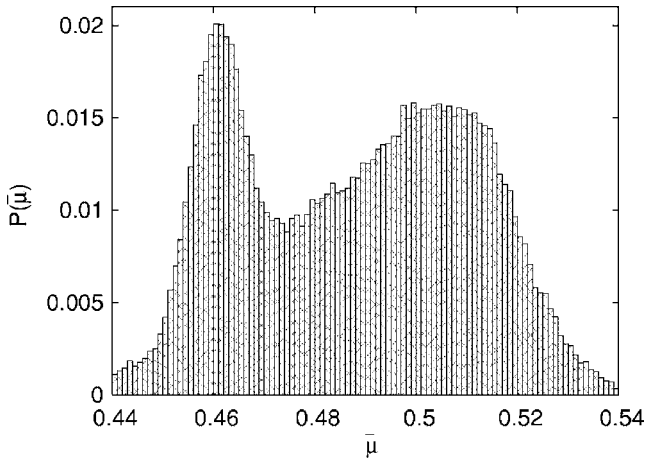

FIG. 3. Distributions of local mean distances, $\bar{\mu}$, between points in the embedded attractor for the kicked double-rotor system. The distribution shows two peaks around the values corresponding to two-dimensional and three-dimensional distributions of points, in agreement with other results on this system confirming the existence of UDV.

tem [19], which has previously been shown to contain UDV [20]. Figure 2 shows a diagram of the kicked double rotor system, which consists of three masses (m_1, m_2, m_2) attached to two massless rods, l_1 and l_2, which pivot at points P_1 and P_2. One of the masses is forced impulsively at periodic intervals, and the system is allowed to evolve continuously in between these "kicks." The motion is assumed to be restricted to a plane and the four-dimensional system can be described by two angles, θ and φ, and the corresponding angular velocities.

A time series was generated by integrating the equations of motion [19] between periodic kicks, and $\sin(\theta)$ was embedded to reconstruct the attractor. This was chosen for the embedding because the angular velocity variables are discontinuous at the kicks [21].

We applied the method described here for the detection of UDV to the embedded data for parameter values when the attractor is known to contain unstable periodic orbits with one and two expanding directions (ρ=5.49, as in Figs. 9(d) and 10(d) in Ref. [20]). In Fig. 3 it can be seen that the corresponding histogram shows definite peaks close to the values $\bar{\mu}$=0.4531 and $\bar{\mu}$=0.5143, as expected in the case of a trajectory visiting regions with one and two unstable dimensions. The spread of the peak for the higher dimensional region is found to be large due to the sparsity of points in this region resulting in statistical broadening. In the following section it will be shown that the method is also suitable for detecting the presence of UDV in time series obtained from experimental measurements.

III. EXAMPLE: SYSTEM OF COUPLED ELECTRONIC OSCILLATORS

A. Description of the configuration

A system of two coupled nonlinear electronic oscillators, the first unit of which is shown schematically in Fig. 4, was used to test the method. The individual units are based on a modification of the van der Pol oscillator circuit [22], each being essentially an autonomous LCR oscillator in parallel to a nonlinear element, P, consisting of a chain of semiconductor diodes. An operational amplifier and a variable resistor provide the control parameters, R_1 and R_2. Data were obtained by measuring the potential difference between the points "V" and "g," which varied approximately between −4.5 and 4.5 V, the magnitudes of which remain unchanged under nondimensionalization. All of the quoted quantities in the following sections are in the nondimensionalized form, where V becomes "x," and "R_1" and "R_2" relate to "α" and "β," respectively. As in any real system, the elements of the circuit are not perfectly balanced, resulting in the two oscillators not being identical, even for the same parameter values.

The system is almost the same as that used by Healey [23], with the exception that the LCR loop has been replaced with a solid state equivalent to eliminate any noise picked up by the inductor coil [24]. Each unit has three degrees of

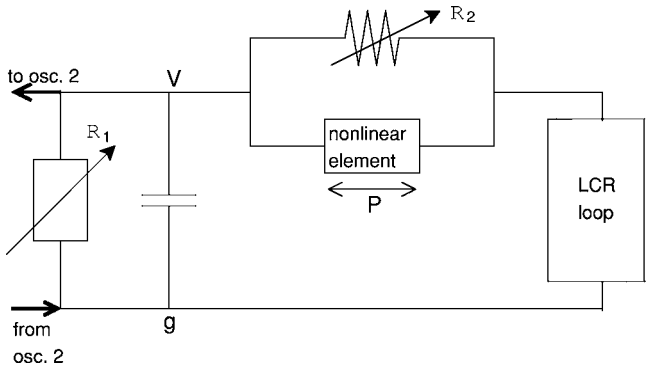

FIG. 4. Circuit based on the van der Pol oscillator. Units are coupled via two unidirectional links from point V of one oscillator to g of the other and vice versa.

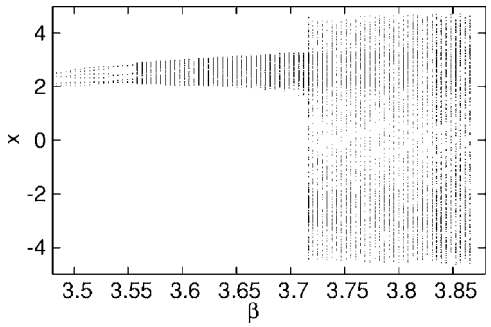

FIG. 5. Bifurcation diagram for the system as a function of the dimensionless parameter β. For $\beta \lesssim 3.72$ there is an almost-symmetric attractor which is not shown. The value x is the first nondimensional embedded coordinate, which is exactly equal in magnitude to the measured voltage response of the system.

freedom and is capable of exhibiting chaotic behavior. When coupled in a loop, in this case by unidirectionally connecting the point V of one oscillator to g of the other and vice versa, the resulting six-dimensional system can present regimes of hyperchaos, as described below. The attractors of the system were reconstructed by embedding measurements of V in a four-dimensional space. This dimension was determined using the false neighbors method [25]. In this work all of the system parameters were kept constant except for β of one of the oscillators. The bifurcation diagram of Fig. 5 shows the evolution of one of the attractors of the system as a function of the parameter β. In the studied range, for values of $\beta < 3.56$ a limit cycle is observed. An almost symmetrical disconnected state can also be found at negative values of x. As β is increased beyond $\beta \approx 3.56$, the limit cycle is seen to develop into a chaotic attractor, which steadily grows in size until $\beta \approx 3.72$, when it experiences an interior crisis and a sudden change in size [26].

At values of β just above this transition, trajectories appear to move intermittently between the two small sets and a large set, the former corresponding to the two attractors present for $\beta \lesssim 3.72$. In Fig. 6 a time series in which trajectories spend appreciable time in each set is shown. This time series is typical of the type of behavior seen when trajectories are split evenly between the different subsets of the attractor. However, at other parameter values it is found that trajectories spend most of their time in a particular region, and such a clear intermittent structure is not observed.

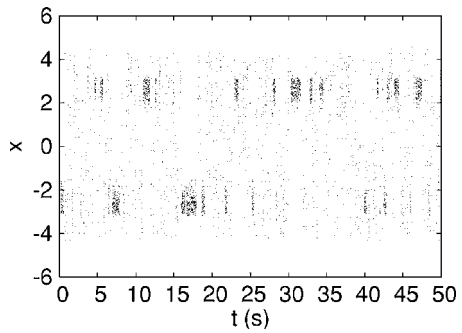

FIG. 6. Time series in a region of parameter space showing clear intermittency between the three sets.

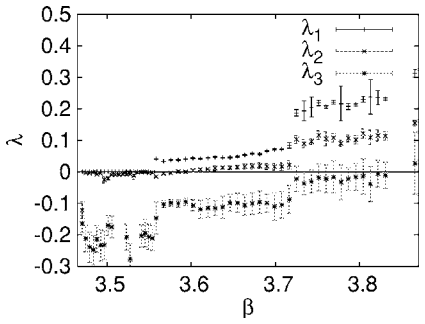

FIG. 7. Evolution of the three largest Lyapunov exponents of the system of coupled oscillators for varying β.

The evolution of the three largest Lyapunov exponents $(\lambda_1, \lambda_2, \lambda_3)$ over the same range of β (Fig. 7) was determined using the method developed by Wolf *et al.* [27] with trajectories containing 2×10^5 points. The errors shown are estimates of the robustness of the method, obtained by varying various parameters of the calculation and observing the resulting shift in the computed values. First, in the limit cycle region of parameter space, we found no positive Lyapunov exponents, as expected. As β was increased a state containing one positive exponent was observed, corresponding to one of the small chaotic sets, as seen in Fig. 5 between $\beta \approx 3.55$ and $\beta \approx 3.72$. At values greater than $\beta \approx 3.72$ there is a transition to a hyperchaotic state with two positive Lyapunov exponents. The transition to hyperchaos approximately coincides in parameter space with the crisis seen in the bifurcation diagram in Fig. 5.

These results suggest that the postcrisis attractor arises from the merger of the two small chaotic attractors, each having one positive Lyapunov exponent, with a larger nonattracting set that has two positive exponents. As the smaller sets contain periodic orbits with one-dimensional unstable manifolds and the larger set periodic orbits with two-dimensional unstable manifolds, a trajectory in the postcrisis attractor will visit the vicinity of periodic orbits with a different number of expanding directions. Thus we expect that the attractor shortly after the crisis will experience UDV. This is confirmed in the following section where we study a model of this physical system.

B. Numerical model

The system described in Sec. III A can be modeled using the following set of equations, that can be derived using Kirchhoff's laws [24]:

$$\frac{dx_1}{d\tau} = \gamma[\beta_1(y_1 - x_1) + f(y_1 - x_1) - \alpha_0 + \alpha_1(x_1 - \epsilon x_2)], \tag{2a}$$

$$\frac{dy_1}{d\tau} = -z_1 - \beta_1(y_1 - x_1) - f(y_1 - x_1), \tag{2b}$$

$$\frac{dz_1}{d\tau} = y_1 - \rho z_1, \tag{2c}$$

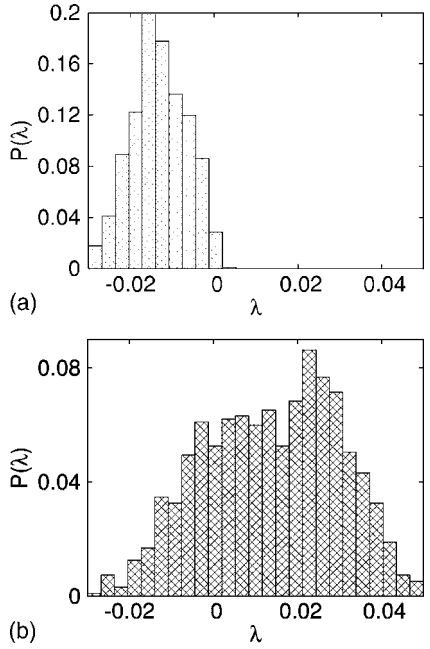

FIG. 8. Histograms of numerically generated short-time Lyapunov exponents. The second and third exponents have been summed to give the peaks shown. The spread of values seen in (b) across positive and negative values is an indication of UDV.

$$\frac{dx_2}{d\tau} = \gamma[\beta_2(y_2 - x_2) + f(y_2 - x_2) - \alpha_0 + \alpha_2(x_2 - \epsilon x_1)], \tag{2d}$$

$$\frac{dy_2}{d\tau} = -z_2 - \beta_2(y_2 - x_2) - f(y_2 - x_2), \tag{2e}$$

$$\frac{dz_2}{d\tau} = y_2 - \rho z_2, \tag{2f}$$

where $f(V) = I_p(e^{kV} - e^{-kV})$ is the voltage response of the nonlinear elements. For oscillators 1 and 2, $x_{1/2}$, $y_{1/2}$, and $z_{1/2}$ are the corresponding independent degrees of freedom, representing dimensionless voltages and currents at various points in the circuit, and $\alpha_{1/2}$ and $\beta_{1/2}$ are the respective variable parameters, which are dimensionless values of variable resistors. The nondimensional time is described by τ, and all other symbols refer to fixed scaling constants. This model gives a good representation of the system for the range of parameters considered in Sec. III A, within the error in determining the scaling constants [24].

The Lyapunov exponents of the system were obtained using the method of Benettin *et al.* [28] and their evolution is very similar to that obtained from the experimental data, confirming that the model and the real system have similar characteristics. Figure 8 shows the histogram of the sum of the second and third STLEs before and after the crisis, for a time of a few periods of oscillation. This sum will take either negative or positive values depending on whether locally there are one or two expanding directions, respectively, as one of these exponents will correspond to the neutral direction of the flow and have a value close to zero. Before the crisis the distribution of this STLE is restricted to negative values [Fig. 8(a)], while shortly after the crisis it includes both positive and negative values [Fig. 8(b)]. As described earlier this indicates that trajectories are visiting regions in the attractor where the number of expanding directions is different.

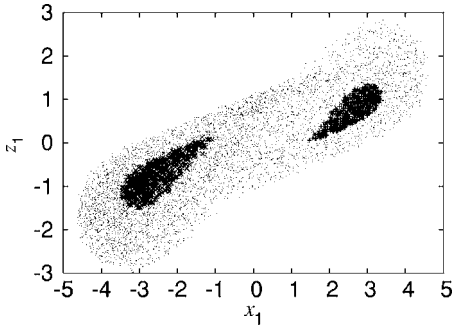

FIG. 9. Two-dimensional projection of periodically sampled orbits of the numerically separated invariant regions. The small sets were found to have one positive Lyapunov exponent and the large set to have two.

We studied in more detail the characteristics of the attractor shortly after the crisis mentioned above by using this model and the PIM-simplex method [29]. The latter allowed us to decompose the attractor into unstable invariant sets and to gain further insight into the origins of UDV in the system. The three invariant sets obtained in this way for parameter values shortly after the crisis are shown in Fig. 9. The points marked with an x correspond roughly to the precrisis attractors, while the larger set indicated with dots is incorporated into the attractor at the point of the crisis. We obtained long trajectories in each of these nonattracting sets and calculated the corresponding Lyapunov exponents using the method of Benettin *et al.* [28]. The small sets were found to only contain one positive Lyapunov exponent and the large set to have two. As all sets are part of the attractor after the crisis, this implies variations in the number of locally expanding directions for points belonging to a typical trajectory.

C. Determination of the local unstable dimension in experimental data

We used the method described in Sec. II to determine the number of expanding directions locally throughout the attractor. The method was applied to time-series data from the system described in Sec. III A at various values of β. The reconstructed attractors consisted of 2×10^5 points embedded in four dimensions. Around each trajectory point x we defined the hyperspherical region $B_\epsilon(x)$, of radius ϵ, to be as small as possible to reduce the effects of curvature, while ensuring that the number of contained points was large enough to obtain good statistics. The optimal size was found to be $\sim 2\%$ of the radius of the attractor. Each hyperspherical region was found to contain from ~ 100 to ~ 2500 points, which we used to determine $\mu(d)$ as described in Sec. II. Averaging was performed over the values of $\mu(d)$ for 20 consecutive points on a trajectory to obtain $\bar{\mu}$ and to reduce

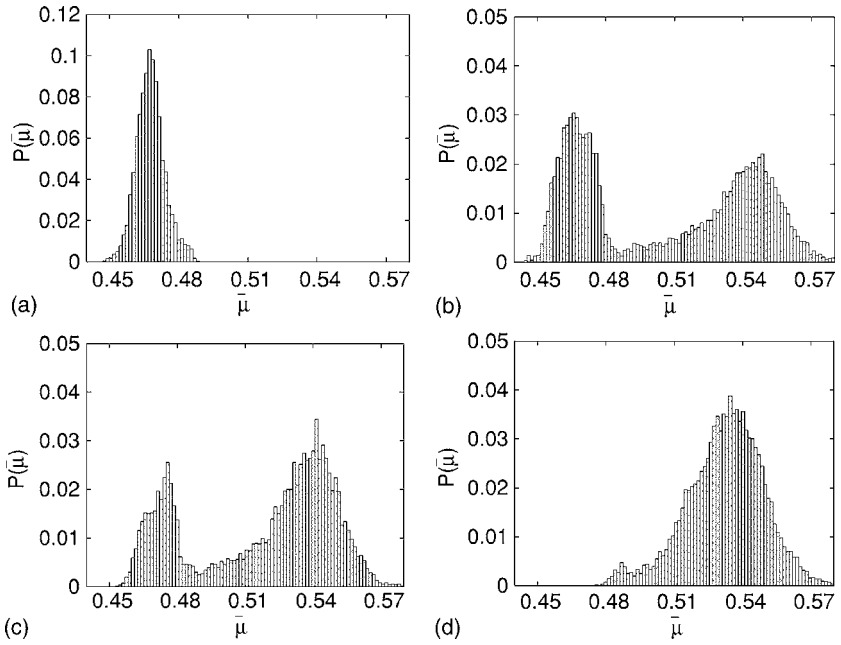

FIG. 10. Distributions of local mean distances, $\bar{\mu}$, between points in the embedded attractor. Before the crisis the values of $\bar{\mu}$ are located around one peak close to the value corresponding to a two-dimensional distribution of points (a). After the crisis, and for nearby values of β, the distribution shows two peaks around the values corresponding to two-dimensional and three-dimensional distributions of points, (b) and (c). For larger values of β the distribution of points is mainly three-dimensional, (d). The values of β for (a), (b), (c), and (d) are 3.69, 3.73, 3.78, and 3.87, respectively.

statistical broadening of the peaks. Histograms at various values of β, showing the distributions of $\bar{\mu}$ over the attractor, both before and after the crisis are presented in Fig. 10. It can be seen clearly that, just before the crisis, the histogram shows only one peak [Fig. 10(a)], with its maximum just above the characteristic value for two dimensions given in Table I. This shows that the reconstructed attractor consists of points which locally lie on a two-dimensional surface everywhere, indicating only one expanding direction to the flow. The small shift of the peak to a value higher than that predicted is believed to be due to the presence of noise and the fractal structure of the attractor along the stable directions, as well as to curvature effects. Noise will cause the contracting directions to be broadened slightly [Fig. 1(b)], separating otherwise nearby points by a small distance and increasing the value of $\bar{\mu}$. This hypothesis was confirmed by performing our method on numerically generated time series of the same system, based on the model described in Sec. III B, both with and without the addition of a small amount of Gaussian noise. It was found that the addition of noise shifted the peak to the right, by an amount related to the magnitude of the noise. However, in the absence of additive noise, the peaks were observed to be slightly lower than the theoretical values. This is probably due to the effects of trajectories passing close to the edge of the attractor, as the neighborhoods of points in this region will be partially empty, resulting in a lower value of the mean distance.

After the crisis, and for parameter values where trajectories were seen to visit the three different sets of the combined attractor, the histograms obtained show two distinct peaks [Figs. 10(b) and 10(c)]. The first recorded peak is at similar values to those recorded before the transition but the second peak has its maximum at a value close to that expected for a three-dimensional distribution of points, indicative of two expanding directions. Thus the trajectory under investigation here is observed to visit regions of phase space where there are both one and two local unstable directions.

The area below each peak gives an idea of the proportion of time the trajectories spend around the one-dimensional and two-dimensional unstable regions. The obstruction to shadowing due to UDV is strongest when each region is visited for a substantial proportion of time as this results in one STLE having large variance and a mean value close to zero [7]. According to Fig. 10 this occurs for β between 3.73 and 3.78. For larger values of β trajectories mainly visit regions with two expanding directions and we can expect fewer changes in the local unstable dimension and longer periods of time where the dynamics can be considered to be nearly hyperbolic.

To compare the effectiveness of the present method with the alternative approaches proposed in the literature, we analyzed the same data using both a technique based on singular value decomposition and on short-time Lyapunov exponents. The method of Broomhead *et al.* [15] studies the singular values of the matrix whose rows consist of the vectors connecting the points in the local region $B_\epsilon(x)$ to its center. The number of significant singular values is expected to be equal to the dimension of the local tangent space, assuming it is well approximated by $B_\epsilon(x)$. However, the presence of noise will give the attractor some thickness in all the contracting directions in phase space. If the radius of the local region, ϵ, is increased beyond the noise threshold, the singular values corresponding to noncontracting directions will increase linearly with ϵ while the singular values of the contracting directions will remain constant until the curvature of the set becomes relevant, thus making it possible to distinguish expanding directions from noisy contracting ones. We applied this technique to the same experimental data studied at the beginning of this section and calculated the singular values at several points along a trajectory on the attractor. Although we considered a range of radii for the local region, in general it was not possible to obtain a clear separation between the significant singular values and those corresponding to noise. This is probably due to the temporal fluctuations of the singular values induced by the presence of dynamical noise [30]. Examples of the calculated singular values, σ_i, are shown in Fig. 11 for part of a trajectory within the embedded

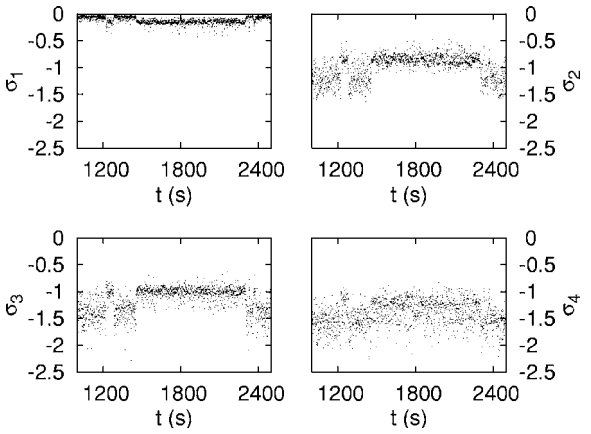

FIG. 11. Singular values, σ_i, at points on a trajectory in the embedded attractor. Although there exist regions where the dimensionality of the attractor is different, the actual dimensionality is difficult to ascertain.

attractor at $\beta=3.78$. The region between $t\approx1500$ and $t\approx2300$ is in the small set with one expanding direction, while the rest is mostly in the larger, higher-dimensional set. The two regions show variations, indicating differences in the dimensionality, but due to the lack of clear separation between the singular values it is impossible to make quantitative estimates of the dimension in either case.

We also calculated the STLEs using the method of Wolf *et al.* [27], which works by finding points aligned with orthogonal directions and following them along a trajectory. These points have to be replaced periodically and with sufficient frequency to ensure that the vectors generated by them stay orthogonal and their size small enough for the linear approximation to remain valid, while also allowing for the expansion and contraction rates to be numerically computable. Although the amount of data we are working with in each neighborhood would appear to be sufficient for this, the random fluctuations in the number of points means that frequently a suitable replacement point cannot be found, making the short time averages less reliable. This is a particular problem when the radius ϵ is reduced to a size necessary for $B_\epsilon(x)$ to be a good approximation to the tangent space of the local manifold, especially in the sparser regions present in the hyperchaotic set. It is also a requirement that one of the vectors be aligned along the direction of the largest STLE, however, this direction is not known *a priori*, so the vectors need to be allowed to evolve for some time before the expansion and contraction rates can be calculated reliably, and this alignment will in general be lost when the trajectory reaches a nonhyperbolic point, thus reducing the actual number of points available to estimate the STLEs. All of these requirements make this technique very sensitive to adjustments to the parameters of the calculation. Although this method works well for the largest STLE, and reasonably for the other positive ones, for the smaller exponents such as the one around zero and particularly for the negative ones, it becomes very unreliable due to a low density of points in the contracting directions. This can be seen by inspecting the second largest STLE of the precrisis attractor at $\beta=3.69$ in Fig. 12(a) [the same parameter value as in Fig. 10(a)] where

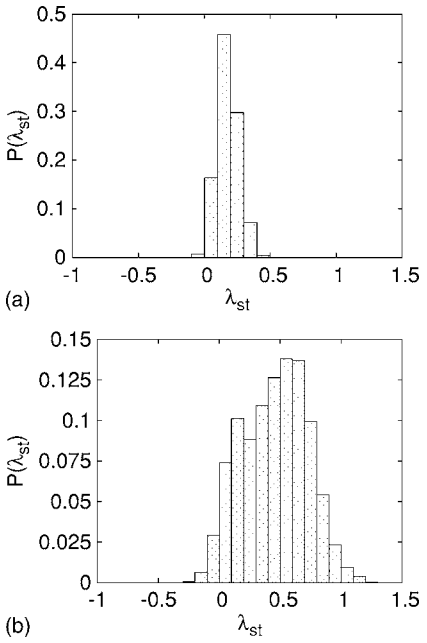

FIG. 12. Histograms of experimentally obtained short-time Lyapunov exponents. The peak shown in (a) shows the second STLE of the precrisis attractor, whereas the second and third exponents of the hyperchaotic attractor have been summed to give the distribution shown in (b).

there is only one expanding direction. This STLE should be zero, but Fig. 12(a) shows that it is difficult to determine this from the values obtained. Figure 12(b) shows the sum of the second and third exponents for $\beta=3.78$, where UDV has already been shown to exist. The histogram shows a spread in the values of these STLEs, but the peak does not clearly cover negative values, as would be needed to positively identify UDV. Thus the only conclusion that can be drawn from this approach is that there exists a variation in the value of the second positive exponent, but it is impossible to distinguish between UDV and a case where there are fluctuations between two purely positive values.

In summary, the calculation of STLEs from experimental data depends very sensitively on the parameters used in the method, making it difficult to estimate accurate values, especially when their magnitude is small. The situation is different in numerical simulations, where the equations of the local tangent flow are known and the STLE can be determined more accurately. Alternative procedures to calculate Lyapunov exponents from experimental data have other limitations, such as the appearance of spurious exponents which need to be identified among the real ones [31]. The method proposed here to establish variations in the local dimension of the set compares the statistics of interpoint distances with tabulated values and appears to be more robust with respect to noise and curvature effects, as well as being less sensitive to variations in the calculation parameters.

Finally, we can also use the information gained from the application of the method to separate the embedded attractor into its regions of different unstable dimension, as shown in Fig. 13 for $\beta=3.77$. Points denoted with crosses correspond to trajectory points where locally there is one expanding di-

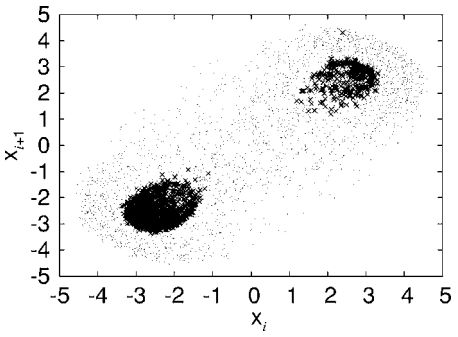

FIG. 13. Projection of the invariant regions within the attractor, reconstructed from experimental data, and separated using information from the application of the method of Sec. II.

rection and those marked with dots to points with a two-dimensional unstable tangent space. Qualitative similarities can be seen between Fig. 13 and the sets obtained by means of the PIM-simplex method in Fig. 9, even though Fig. 13 is for a four-dimensional embedding in a different projection to the six dimensional simulation of Fig. 9. While in Sec. III B we relied on numerical computations and the availability of a model of the physical system, here the same information was obtained solely from the experimental data.

IV. SUMMARY AND DISCUSSION

Unstable dimension variability has been shown in recent years to be a crucial factor in determining shadowing times in systems with more than three degrees of freedom. Here we have presented a method to detect the presence of UDV in experimental data. The procedure relies on the distribution of trajectories in the reconstructed attractor and does not require the calculation of short-time Lyapunov exponents. We showed that the method gives enough information to allow us to decompose the attractor into invariant unstable subsets with different numbers of positive Lyapunov exponents, and to determine the proportion of time a typical trajectory spends in each.

The proposed method only requires the calculation of distances between pairs of points, and as a consequence it is very easy to implement. As with other techniques, the presence of noise has a detrimental effect but in the cases studied this method appears to be robust enough to yield useful information. In particular, small amounts of noise will induce a shift of the peaks in the histogram of $\bar{\mu}$ to higher values, giving the possibility of using the method as a tool for measuring the dynamical noise in a system as compared to the model situation.

Another limiting factor we can conceive of is when the shadowing times become exceptionally short. In cases where the time a trajectory spends in regions with constant unstable dimension is shorter than the number of steps over which a useful average can be obtained for $\bar{\mu}$ (which can be taken as less than the length of a few typical orbital periods) the method will fail. However, in such cases trajectories will have little or no time to spread or converge into the new expanding or contracting subspaces and the attractor in such cases will exhibit no clear dimension.

In this work we applied our method to a real system with six degrees of freedom but we believe it to be robust enough to be effective in systems of higher dimension. As the dimension under investigation increases, so will the size of the time series needed to obtain enough embedded points for the method to succeed. Because it is based on the statistics of distances between pairs of points, the required size of the local data set, N, is expected to scale in a similar manner to that needed for calculations of the correlation dimension, which has been shown to scale as $N \sim 10^{\nu/2}$, where ν is the dimension of the set [32]. In that same work, the amount of data required for the calculation Lyapunov exponents was shown to be approximately the square of that for the correlation dimension. Another limiting factor is that the theoretical values for the average interpoint distance μ asymptotes towards $\sqrt{2}$ as the dimension approaches infinity. Despite this, the method described here appears to be more robust with respect to noise, curvature, and limited amounts of data than the other methods proposed in the literature to obtain the local dimension of the unstable set in the attractor. We believe the method will be successful for systems in which UDV cannot be determined by other means. Thus we expect it to be a useful tool in the study of systems with moderate and high number of degrees of freedom where UDV is more prevalent, such as those arising from reductions to inertial manifolds in systems of partial differential equations. In those cases the method would be valuable for identifying nonattracting sets and determining their role in phenomena such as turbulence and spatiotemporal chaos.

ACKNOWLEDGMENTS

N.J.M. gratefully acknowledges the support of the Engineering and Physical Sciences Research Council (EPSRC). We are also grateful to the Electronics Workshop of the School of Physics and Astronomy, University of Manchester, and especially Mike Needham, for the construction of the high quality electronic circuits used in this study.

[1] J. Guckenheimer and P. Holmes, *Nonlinear Oscillations, Dynamical Systems and Bifurcations of Vector Fields* (Springer-Verlag, 1983).

[2] Y.-C. Lai, C. Grebogi, J. A. Yorke, and I. Kan, Nonlinearity **6**, 779 (1993).

[3] Y.-C. Lai, D. Lerner, K. Williams, and C. Grebogi, Phys. Rev. E **60**, 5445 (1999).

[4] A. D. Ansov, Proc. Steklov Inst. Math. **90**, 1 (1967); R. Bowen, J. Diff. Eqns. **18**, 333 (1975).

[5] S. M. Hammel, J. A. Yorke, and C. Grebogi, J. Complex. **3**,

136 (1987); Bull., New Ser., Am. Math. Soc. **9**, 465 (1988); C. Grebogi, S. M. Hammel, J. A. Yorke, and T. Sauer, Phys. Rev. Lett. **65**, 1527 (1990); T. Sauer and J. A. Yorke, Nonlinearity **4**, 961 (1991); S. N. Chow and K. J. Palmer, J. Dyn. Differ. Equ. **3**, 361 (1991); S. N. Chow and E. S. van Vleck, SIAM J. Sci. Comput. (USA) **15**, 959 (1994).

[6] S. Dawson, C. Grebogi, T. Sauer, and J. A. Yorke, Phys. Rev. Lett. **73**, 1927 (1994).

[7] T. Sauer, C. Grebogi, and J. A. Yorke, Phys. Rev. Lett. **79**, 59 (1997).

[8] E. J. Kostelich, I. Kan, C. Grebogi, E. Ott, and J. A. Yorke, Physica D **109**, 81 (1997); Y.-C. Lai and C. Grebogi, Phys. Rev. Lett. **82**, 4803 (1999); E. Barreto and P. So, *ibid.* **85**, 2490 (2000); T. D. Sauer, Phys. Rev. E **65**, 036220 (2002).

[9] H. D. I. Abarbanel, R. Brown, J. J. Sidorowich, and L. S. Tsimring, Rev. Mod. Phys. **65**, 1331 (1993).

[10] F. Takens, *Detecting Strange Attractors in Turbulence*, Lecture Notes in Math. Vol. 898 (Springer, New York, 1981).

[11] D. S. Broomhead and G. P. King, Physica D **20**, 217 (1986).

[12] H. W. Hirsch and C. C. Pugh, Proc. Symp. Pure Math. **14**, 133 (1970).

[13] D. Ruelle, Suppl. Prog. Theor. Phys. **64**, 339 (1978).

[14] H. Froehling, J. P. Crutchfield, D. Farmer, N. H. Packard, and R. Shaw, Physica D **3**, 605 (1981).

[15] D. S. Broomhead, R. Jones, and G. P. King, J. Phys. A **20**, L563 (1987).

[16] T. Hediger, A. Passamante, and M. E. Farrell, Phys. Rev. A **41**, 5325 (1990).

[17] J. M. Hammersley, Ann. Math. Stat. **21**, 447 (1950).

[18] R. S. Bennett, IEEE Trans. Inf. Theory **IT-15**, 517 (1969).

[19] C. Grebogi, E. Kostelich, E. Ott, and J. A. Yorke, Physica D **25**, 347 (1987).

[20] P. Moresco and S. P. Dawson, Phys. Rev. E **55**, 5350 (1997).

[21] Due to the large variations in the density of points between the different regions of the attractor, we found it necessary both to generate a large time-series (to "fill-out" the sparser, high-dimensional regions) and to take a random sampling of points in neighborhoods where the density was very high (to quicken calculation in the high-density. low-dimensional regions).

[22] B. van der Pol, London, Edinburgh Dublin Philos. Mag. J. Sci. **3**, 65 (1927).

[23] J. J. Healey, D. S. Broomhead, K. A. Cliffe, R. Jones, and T. Mullin, Physica D **48**, 332 (1991).

[24] P. Kerr-Delworth, Ph.D. thesis, University of Manchester, 1999.

[25] M. B. Kennel, R. Brown, and H. D. I. Abarbanel, Phys. Rev. A **45**, 3403 (1992).

[26] Due to the imperfect symmetry of the system the two small attractors experience the crisis at slightly different values of β.

[27] A. Wolf, J. B. Swift, H. L. Swinney, and J. A. Vastano, Physica D **16**, 285 (1985).

[28] G. Benettin, L. Galgani, A. Giorgilli, and J.-M. Strelcyn, Meccanica **15**, 9 (1980).

[29] P. Moresco and S. P. Dawson, Physica D **126**, 38 (1999).

[30] M. Todoriki, H. Nagayoshi, and A. Suzuki, Phys. Rev. E **72**, 036207 (2005).

[31] T. D. Sauer, J. A. Tempkin, and J. A. Yorke, Phys. Rev. Lett. **81**, 4341 (1998).

[32] J.-P. Eckmann and D. Ruelle, Physica D **56**, 185 (1992).